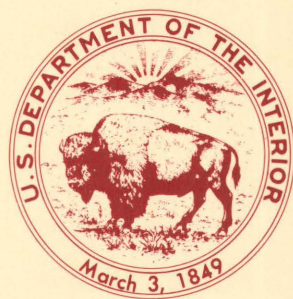


Development of a Velocity Model for
Locating Aftershocks in the
Sierra Pie de Palo Region of
Western Argentina

U.S. GEOLOGICAL SURVEY BULLETIN 1795



Development of a Velocity Model for Locating Aftershocks in the Sierra Pie de Palo Region of Western Argentina

By G. A. Bollinger and C. J. Langer

Local extreme variations in sedimentary thickness required development of a velocity model to accurately compute hypocenters of the aftershock seismicity following the western Argentina (Caucete) earthquake of November 23, 1977.

DEPARTMENT OF THE INTERIOR
DONALD PAUL HODEL, Secretary

U.S. GEOLOGICAL SURVEY
Dallas L. Peck, Director



UNITED STATES GOVERNMENT PRINTING OFFICE, WASHINGTON: 1988

For sale by the
Books and Open-File Reports Section
U.S. Geological Survey
Federal Center
Box 25425
Denver, CO 80225

Library of Congress Cataloging-in-Publication Data

Bollinger, G. A.

Development of a velocity model for locating aftershocks in
the Sierra Pie de Palo region of western Argentina.

(U.S. Geological Survey bulletin ; 1795)

Bibliography: p.

Supt. of Docs. no.: I 19.3:1795

1. Seismology—Argentina—Pie de Palo Mountains Region.

I. Langer, C. J. II. Title. III. Series

QE75.B9 no.1795 557.3 s 87-600225

[QE535.2A7] [551.2' 2' 098263]

CONTENTS

| | |
|---|----|
| Abstract | 1 |
| Introduction | 1 |
| Regional geologic setting | 1 |
| Development of velocity model and travel time corrections | 3 |
| Summary | 12 |
| Acknowledgments | 13 |
| References cited | 13 |
| Appendix | 14 |

FIGURES

| | |
|--|----|
| 1. Aftershock epicenter map | 2 |
| 2. Location map of study area | 3 |
| 3. Locations of refraction profiles | 4 |
| 4. Thickness of sedimentary rocks | 6 |
| 5. Average sedimentary rock velocities | 7 |
| 6. Uppermost Precambrian rock velocities | 8 |
| 7. Grid map for velocities and thickness | 9 |
| 8. Sedimentary rock travel times | 10 |
| 9. Wadati diagram | 12 |

TABLES

| | |
|---|----|
| 1. P-wave velocity model, Sierra Pie de Palo region of Western Argentina | 11 |
| 2. Velocity model (AVM) station corrections, T_c , Argentina aftershock network | 11 |
| 3. Station-delay corrections, T_d , Argentina aftershock network | 12 |
| 4. Final station corrections, T_s , Argentina aftershock network | 12 |

Development of a Velocity Model for Locating Aftershocks in the Sierra Pie de Palo Region of Western Argentina

By G. A. Bollinger¹ and C. J. Langer

Abstract

The ten stations included in a temporary seismograph network for locating aftershocks of the November 23, 1977, western Argentina earthquake were sited where the underlying sedimentary rock columns had thicknesses ranging from 0 to 6 km (up to 1.5-sec variation in vertical one-way travel times for the P-waves). Such rapid changes in the velocity structure cause considerable difficulty in obtaining accurate hypocenter locations. Fortunately, velocity data were available in the form of 26 refraction profiles for the near surface (0–6+ km). Those profiles gave the velocities for the sedimentary column and the underlying Precambrian basement in the network area. An estimate of the regional crustal velocity structure for this geologically complex area had also been determined previously by analysis of data from a well-located nearby earthquake. Unpublished surface-wave studies extend the model to the upper mantle. This paper describes the use of the available data to refine the velocity estimates for the uppermost layers of the regional crustal velocity model and the method used to calculate P-wave travel time corrections for each station. The resulting model and station corrections were used, with good results, to locate the 185 aftershocks listed in the appendix. Average HYPO71 error measures for the aftershock hypocenters were: RMS=0.12 sec, ERH=0.7 km, ERZ=1.3 km.

INTRODUCTION

The epicentral region for the magnitude 7.3 (M_s) western Argentina (Caucete) earthquake of November 23, 1977, and its aftershocks is restricted primarily to the eastern half of the Sierra Pie de Palo and to the eastern adjoining Valle Bermejo (fig. 1). That area lies within the Sierras de las Pampeanas (fig. 2) and is associated with the Sierras Pampeanas Occidentales geologic province,

a region of considerable stratigraphic and structural complexity (e.g., see Allmendinger and others, 1983; INPRES, 1977; Bastias and Weidmann, 1983; Jordan and others, 1983). The resulting velocity structure varies rapidly in both the horizontal and vertical directions; consequently, the area poses serious problems to accurate earthquake hypocentral locations.

The following discussion presents a brief summary of the regional geology of the aftershock zone followed by a detailed description of a four-stage procedure used to construct a local velocity model for the aftershock locale. Development of individual station corrections to account for systematic travel time differences at each of the seismograph locations completed the velocity model study.

REGIONAL GEOLOGIC SETTING

The Sierra Pie de Palo is encircled by a system of broad valleys (Valle del Bermejo to the east and Valle de Tulum to the south and west) that form a doughnut-shaped basin (elevation of 500–700 m) filled in places with several kilometers of Quaternary age sediments. The eastern neighboring mountains, Sierra de la Huerta and Sierra de Valle Fertil as well as the central Sierra Pie de Palo, are composed of Precambrian and lower Paleozoic metamorphic and intrusive rocks that rise to more than 3,000 m above sea level. The mountain fronts are generally bounded by northerly or north-northwest-striking reverse faults that dip moderately to the east (Jordan and others, 1983; Bastias and Weidmann, 1983) but a set of crosscutting, east-northeast-trending faults and lineaments are also present (INPRES, 1977, p. 13). West of the Sierra Pie de Palo are the Paleozoic highlands that form the Andean Precordillera Centro Occidental with elevations locally in excess of 4,000 m. Reverse faulting here is extensive along both east- and west-dipping

¹USGS and Virginia Polytechnic Inst. and State University, Blacksburg, Virginia 24061.

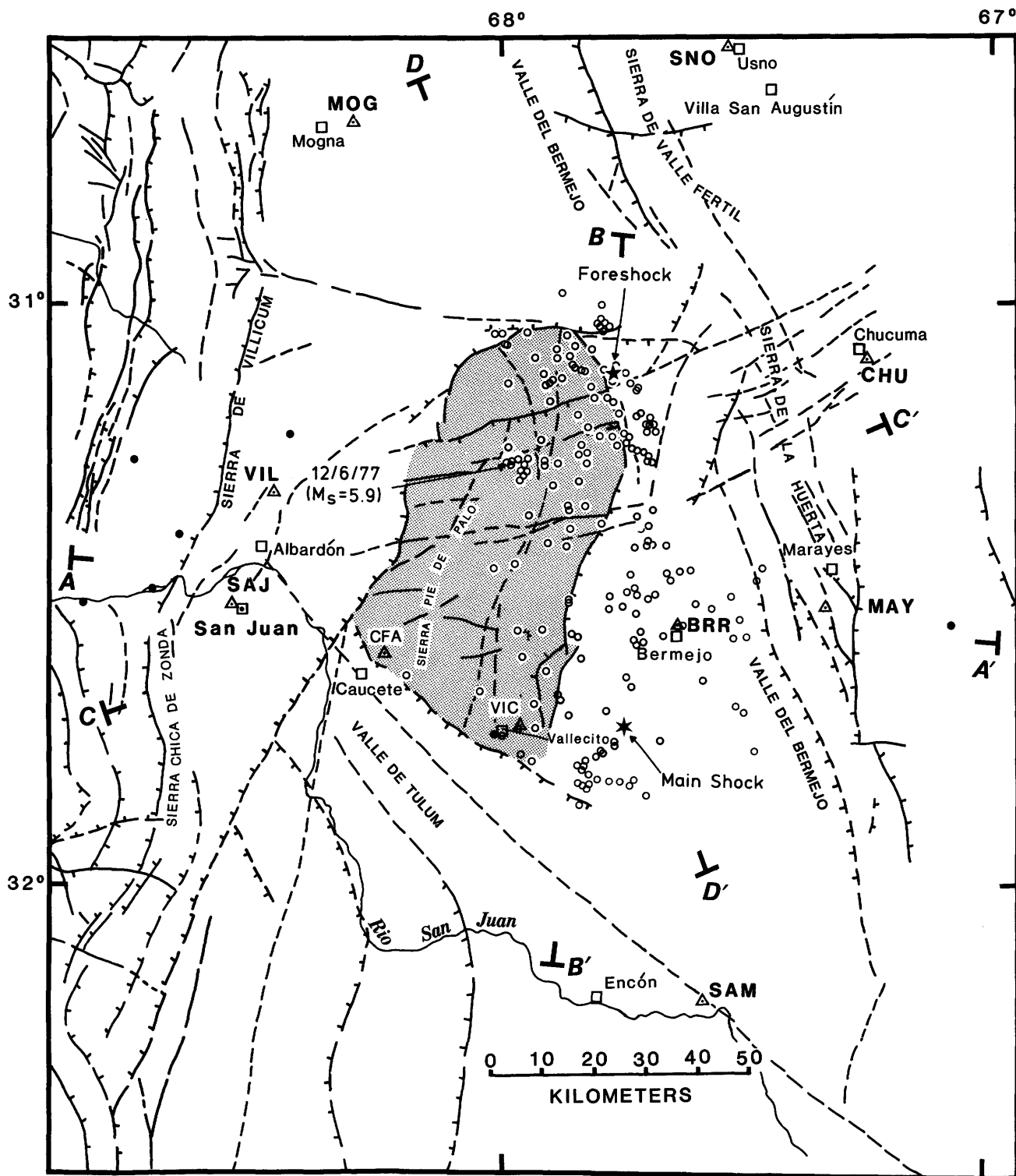


Figure 1. Aftershock epicenter (open circles) map after Langer and Bollinger (1987). Foreshock epicenter (five-pointed star) and main shock epicenter (solid six-pointed star) are from Kadinsky-Cade and others (1985); station locations shown by open triangles with center dot and three-letter station codes. Intermediate depth earthquake epicenters indicated by solid dots. Note that two of these deeper events are off the west side of the figure. Faults, shown by heavy solid (confirmed) or dashed (inferred) lines with hachures on down-dropped sides, and Precambrian outcrop on the Sierra Pie de Palo, shown by pattern symbols, were taken from INPRES (1977) geologic map. Cities and villages are indicated by open square symbols and names.

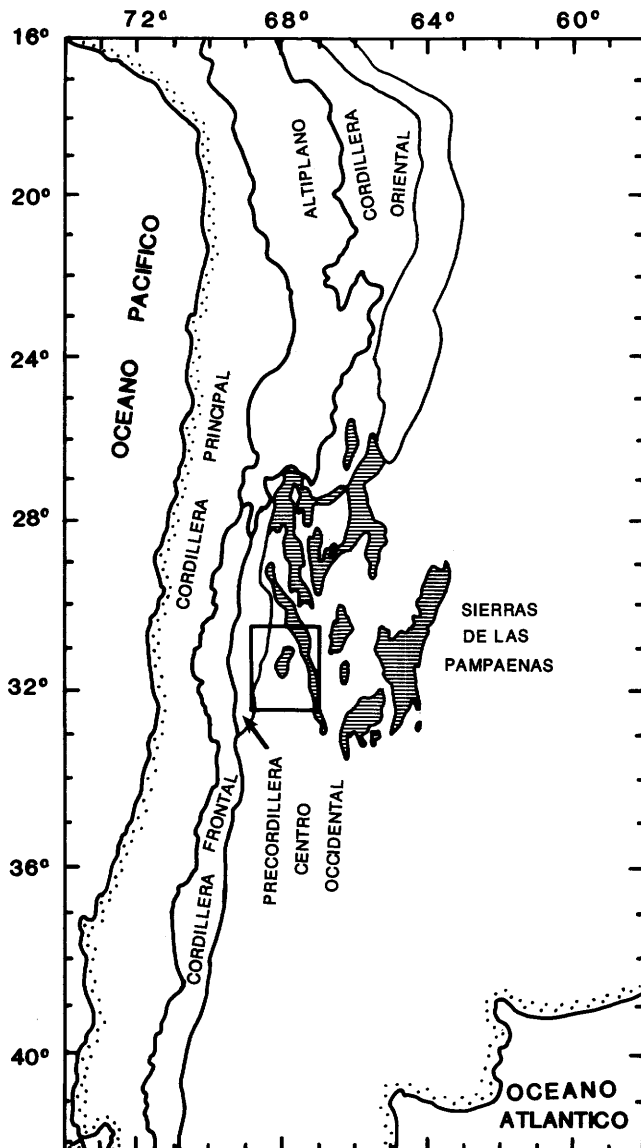


Figure 2. Location map of study area (rectangle) showing some of the geologic provinces of western Argentina. Irregularly shaped patterned figures are Sierras de las Pampaeas. The map is modified from Jordan and others (1983).

faults that predominantly strike north-south, subparallel to the Andean front. Bastias and Wiedmann (1983) have examined and described some of the major faults both east and west of Sierra Pie de Palo and have documented evidence for Holocene movement on several of the fault scarps. Baldis and Febrer (1983) have suggested that the north-northwest-striking faults just east of the Sierra Pie de Palo and the east-northeast crosscutting faults through the Sierra Pie de Palo (fig. 1) represent intersecting megafault systems that have been active from early Precambrian time to present.

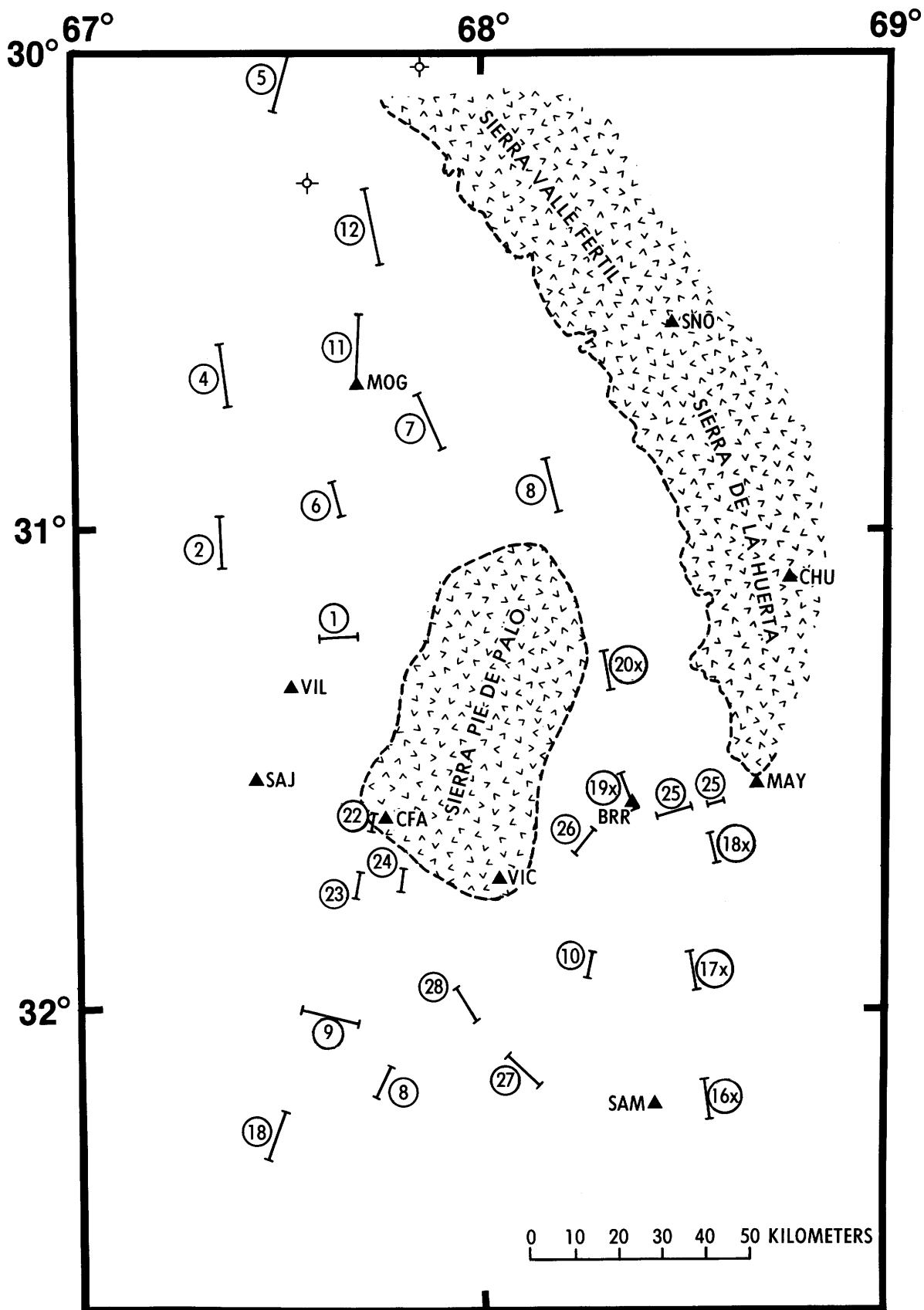
DEVELOPMENT OF VELOCITY MODEL AND TRAVEL TIME CORRECTIONS

The network of eight portable and two permanent stations used to record the aftershock activity of the November 23, 1977, earthquake resulted in five stations being sited on Precambrian rocks (CFA, VIC, MAY, CHU, and SNO) and five stations on the basinal alluvium (MOG, BRR, SAM, VIL, and SAJ; e.g., see fig. 3). Given these very different station bedrock types, fortunately an approximate regional P-wave crustal-velocity model (Volponi, 1968) and results from 26 refraction profiles in the epicentral area were made available by Yacimientos Petroliferos Fiscales (YPF), the Argentine National Oil Company (see fig. 3). All but one of the YPF profiles were reversed and provided data to compute the sedimentary column and uppermost Precambrian (basement) velocities. Additionally, sonic log data from two wells that had been drilled in the northern part of the study area near 30°S., 68°W. (D. R. Toland, Cities Service Company, Houston, Tex., personal commun., 1978; fig. 3) agreed, generally, with the refraction velocity data in their vicinity. However, the wells were not drilled deep enough to extend our knowledge of the Precambrian velocities and, thus, only helped to confirm the velocity information within the section. Also, depth to the top of the mantle (Mohorovičić discontinuity), and the upper mantle velocity were estimated by J. C. Castano (staff seismologist, INPRES, San Juan, Argentina, personal commun., 1977) based on unpublished surface-wave studies.

To correct for the complexities in lithology and the other local geologic factors that affect seismic velocities, we state the following objectives and the analytic procedures to achieve these objectives:

- Develop an “average” layered velocity model (AVM) that is representative of the upper 10 km of crust in the Sierra Pie de Palo area.
- Estimate station corrections to account for systematic travel time differences at each station that result from the model.
- Estimate “station-delay” corrections that account for systematic travel time differences at each station that result from unknown sources.
- Combine the AVM station corrections with the “station-delay” corrections to estimate the “final” station corrections.

A brief summary of what the available data include is: 25 reversed and 1 non-reversed refraction profiles, well log data from 2 wells, a regional velocity model (Volponi, 1968), depth to the upper mantle and upper mantle velocity estimates from Castano, and aftershock data recorded at 10 stations. Our task is to apply these data



in a rational and also rigorous method to achieve the above-stated goals. A step-by-step description of how the "average velocity model" was developed and how the station corrections were determined is given below.

(1) *Average velocity model (AVM), Upper 10 km*

- (a) Location, length, and direction of profiles were plotted (fig. 3).
- (b) Thickness and average sedimentary-column velocities were determined for all profiles, plotted at the profile center, and contoured (figs. 4 and 5).
- (c) Precambrian basement velocities were determined, found to be variable, plotted, and contoured (fig. 6).
- (d) The study area was gridded at 1/4-degree intervals and, for each of the resulting 45 grid points, the sedimentary velocity (V_{sed}), sedimentary thickness (Z_{sed}), and Precambrian basement velocity (V_{pe}), were estimated by interpolation between respective contours and then plotted (fig. 7).
- (e) Mean values were obtained directly for each of the parameters in figure 7 and used as representative numbers in the AVM. The generalized P-wave velocity model for the upper 10 km is then:

| P-wave Velocity (km/sec) | Thickness (km) | Depth to top of layer (km) |
|--------------------------|----------------|----------------------------|
| 2.87 | 2.4 | 0 |
| 5.88 | 7.6 | 2.4 |

Available measurements of middle and lower crustal velocities from Volponi (1968) add to our model and are as follows:

| P-wave Velocity (km/sec) | Thickness (km) | Depth to top of layer (km) |
|--------------------------|----------------|----------------------------|
| 6.2 | 22.0 | 10.0 |
| 7.3 | ? | ? |

The combination of our AVM with Volponi's investigation (1968) and information from J. C. Castano leads to our final P-wave velocity model given in table 1.

The model specifies only average velocities and thicknesses for the two layers above 10 km. However, looking at figures 4-8, considerable variability exists in sedimentary thickness, sedimentary velocity, and Precambrian velocity throughout the network area. Given the velocity and thickness for the AVM layers and, then, using figures 4, 5, and 6, to determine the "actual" P-wave travel time parameters for the upper two layers, we can estimate the AVM station corrections.

(2) *AVM Station Corrections, T_c*

- (a) Determine vertical, one-way travel time through the upper 10 km which we call the "AVM travel time," T_m , according to values specified by the AVM.
 $T_m = (2.4 \text{ km}/2.87 \text{ km/sec}) + (7.6 \text{ km}/5.88 \text{ km/sec}) = 0.84 \text{ sec} + 1.29 \text{ sec} = 2.13 \text{ sec}$
- (b) Use the "AVM travel time" ($T_m = 2.13 \text{ sec}$) to contrast with the "actual station travel times," T_a , at each of the network stations.
- (c) Calculate difference between AVM and "actual" travel times for AVM station corrections:

$$T_c = T_m - T_a$$

Sample AVM station correction calculations are given below for a basin location (MOG) and rock location (MAY). Because of adjustments in scale and projection that were necessary to composite the several large work maps used for preparation of the illustrations, corrections derived directly from the figures presented herein may not agree exactly with those described in the following text.

T_c for MOG (Sedimentary Site)

- a. From figure 8, the sedimentary travel time, $T_{sed} = 1.8 \text{ sec}$
- b. From figure 3, the sedimentary thickness (including station elevation), $Z_{sed} = 6.2 \text{ km}$
- c. From figure 6, the Precambrian velocity, $V_{pe} = 6.0 \text{ km/sec}$
- d. Thickness of Precambrian above 10 km, $Z_{pe} = 10.0 - Z_{sed} = 10.0 \text{ km} - 6.2 = 3.8 \text{ km}$

Figure 3. (facing page) Location of refraction profiles obtained from Yacimientos Petroliferos Fiscales (YPF) (Burna, Abel E., Ing., Chief, Special Studies Agency of Interpretation and Investigation, YPF, Buenos Aires, Argentina, written commun., 1978); profiles are indicated by short lines with end bars; profile numbers given inside open circle symbols are those assigned by YPF. Seismograph station locations shown by solid triangles and 3-letter station codes. Location of two wells indicated by dry-hole symbols (open circles with four tic marks). Precambrian outcrop areas shown by pattern symbol. Open area, except to the far west, represents basinal sediments.

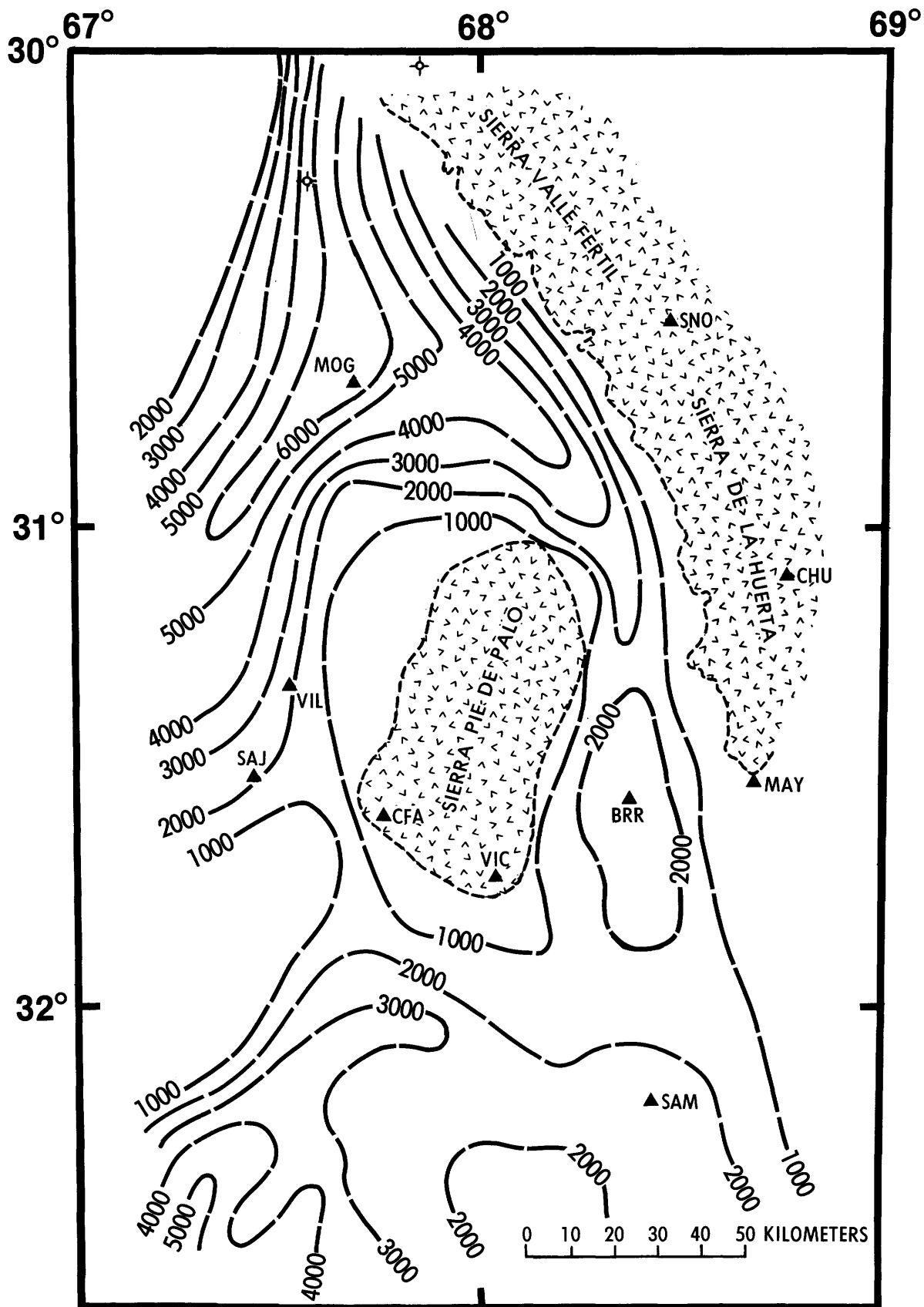


Figure 4. Thicknesses of sedimentary rocks, as calculated from the refraction profile data (fig. 3), contoured in meters. Other symbols the same as in figure 3.

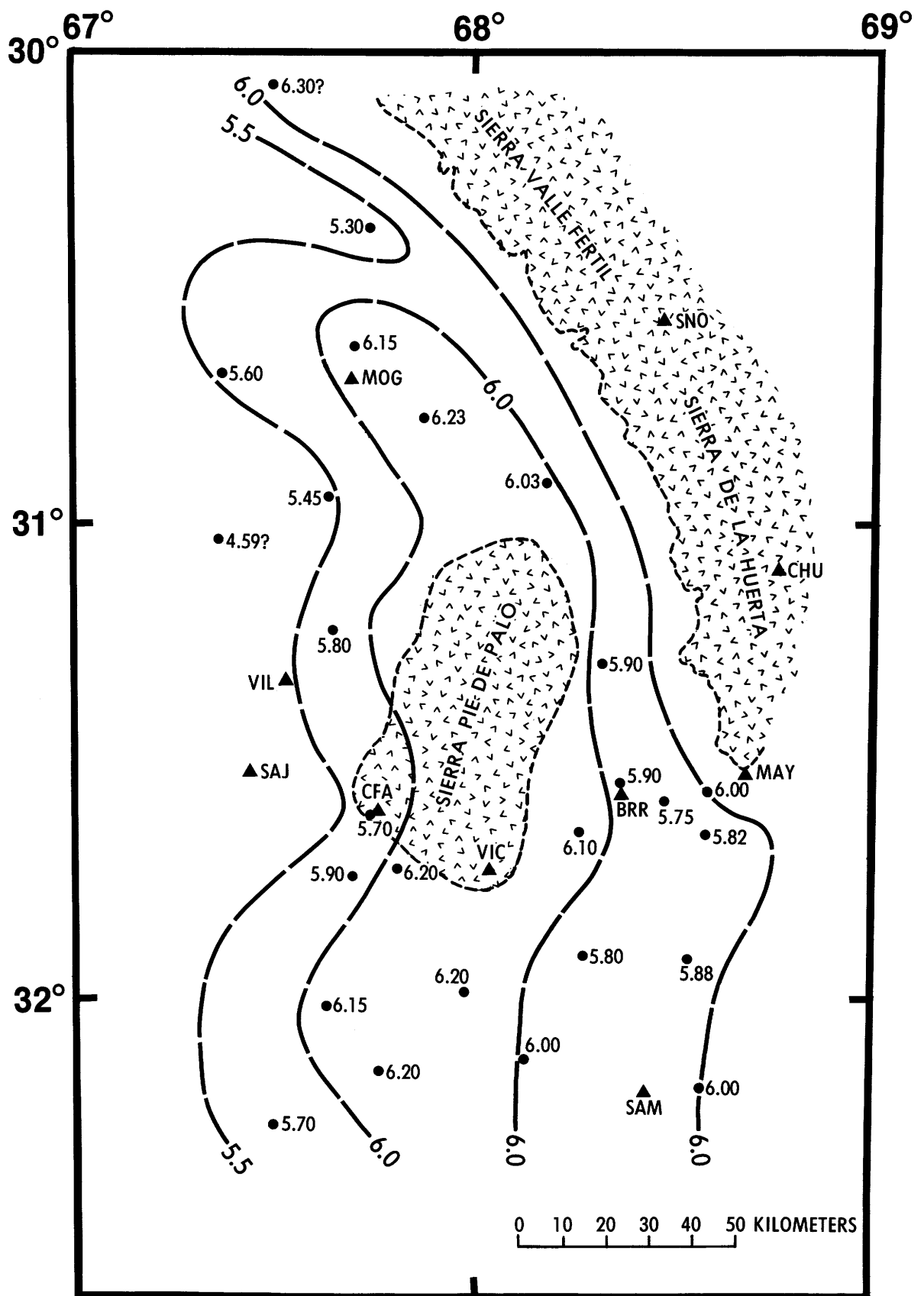


Figure 6. Uppermost Precambrian rock velocities, as determined by the refraction profile data (fig. 3), contoured in km/sec. Other symbols the same as in figure 3.

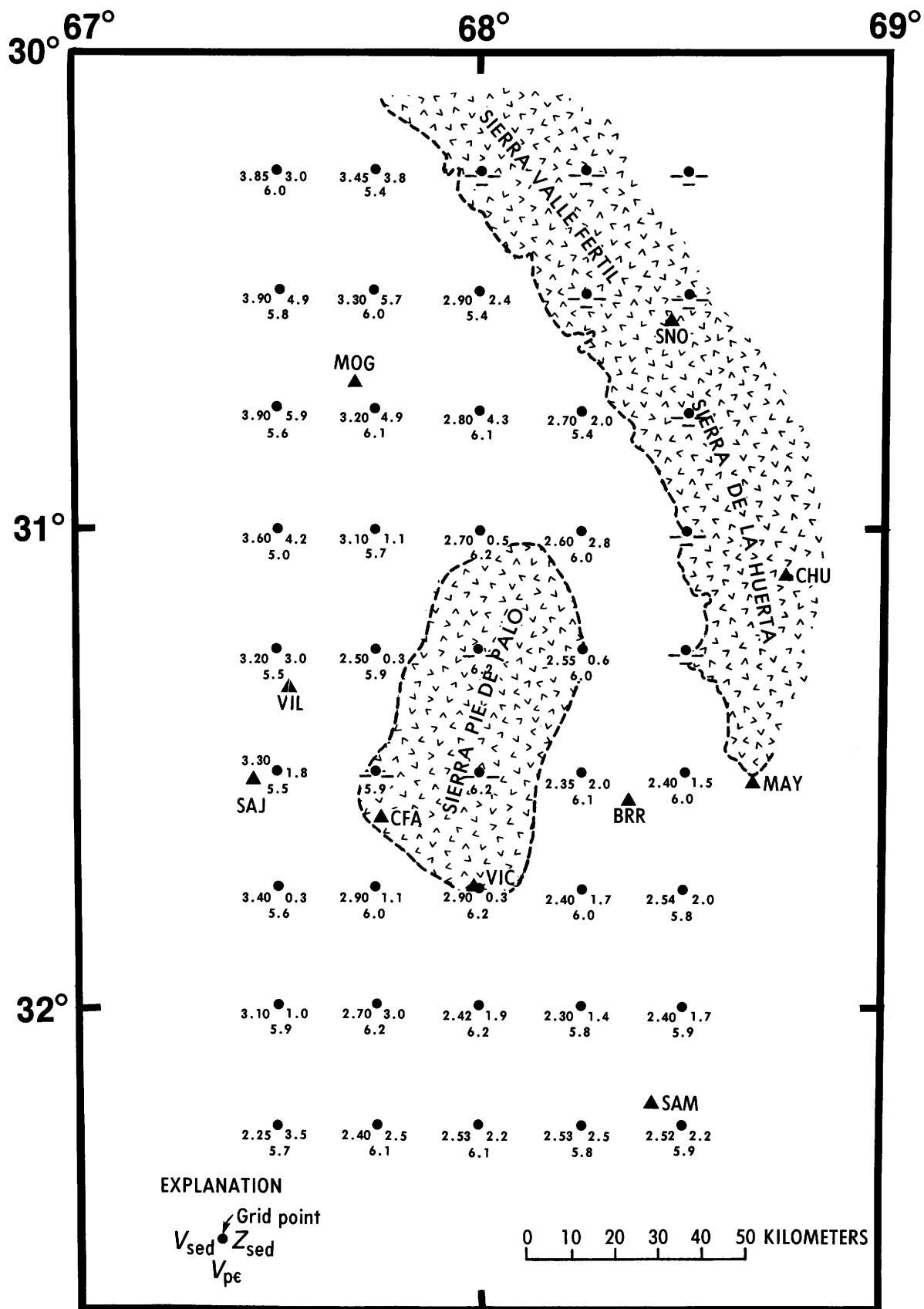


Figure 7. Grid map for velocities (sedimentary rocks = V_{sed} , Precambrian rocks = V_{pe} , both in km/sec) and sedimentary rock thicknesses (Z_{sed} , in km), as derived from figures 4, 5, and 6. Other symbols same as in figure 3.

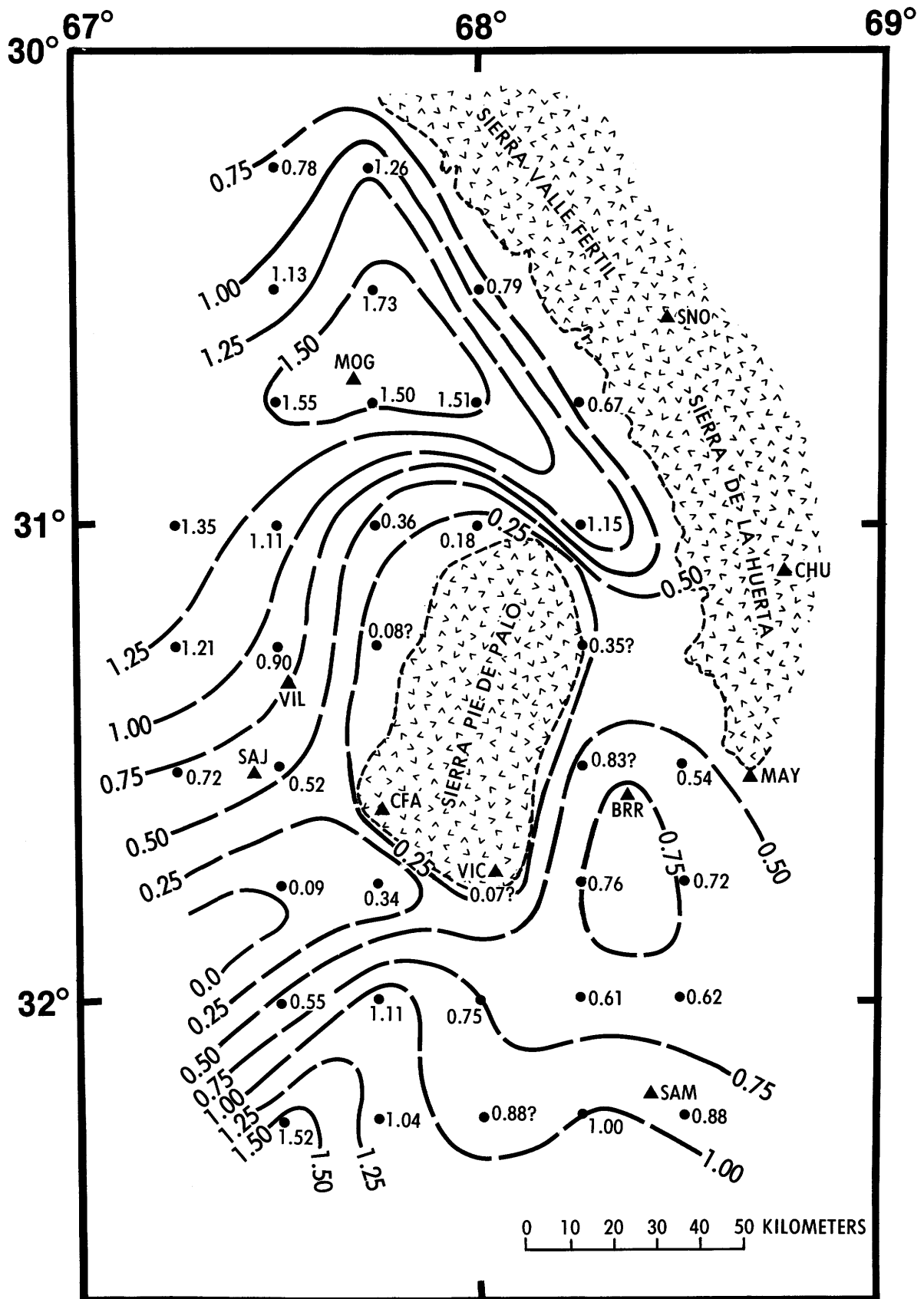


Figure 8. Sedimentary rock traveltimes (one-way vertical path), as calculated from the data shown in figures 4 and 5, contoured in seconds. Other symbols the same as figure 3.

Table 1. P-wave velocity model, Sierra Pie de Palo region of western Argentina

| P-wave velocity (km/sec) | Thickness (km) | Depth to top of layer (km) |
|-----------------------------|-------------------|-------------------------------|
| 2.87 | 2.4 | 0 |
| 5.88 | 7.6 | 2.4 |
| 6.2 | 22.0 | 10.0 |
| 7.3 | 23.0 | 32.0 |
| 8.1 | half-space | 55.0 |

- e. Precambrian travel time, $T_{pe} = Z_{pe}/V_{pe} = 3.8$ km/6.0 km/sec = 0.63 sec
- f. "Actual" one-way travel time, $T_a = T_{sed} + T_{pe} = 1.80$ sec + 0.63 sec = 2.43 sec
- g. Station correction, $T_c = T_m - T_a = 2.13$ sec - 2.43 sec = -0.30 sec

T_c for MAY (Rock Site)

- a. From figure 8, the sedimentary travel time, $T_{sed} = 0.0$ sec (station located on Precambrian rock)
- b. Sedimentary thickness, $Z_{sed} = 0.0$
- c. From figure 6, the Precambrian velocity, $V_{pe} = 6.0$ km/sec
- d. Thickness of Precambrian above 10 km, $T_{pe} = 10.0$ km + station elevation = 10.0 km + 0.71 km = 10.71 km
- e. Precambrian travel time, $T_{pe} = Z_{pe}/V_{pe} = 10.71$ km/6.0 km/sec = 1.78 sec
- f. "Actual" one-way travel time, $T_a = T_{sed} + T_{pe} = 0.0$ sec + 1.78 sec = 1.78 sec
- g. Station correction, $T_c = T_m - T_a = 2.13$ sec - 1.78 sec = +0.35 sec

A listing of the corrections derived in a similar manner for all network stations is given in table 2.

(3) *Station-delay Corrections, T_d*

The AVM station corrections almost certainly will not account for all of the travel time complexities within the region. Therefore, "station delay corrections," T_d , determined from the travel time residuals will also be applied in this study. Those corrections were calculated using the following procedure:

- a. Select a 20-event subset from the entire sample of aftershocks of the November 23, 1977, Argentina earthquake that were recorded by the portable network. Those 20 events should be well recorded by all of the network stations and have epicenters that are well distributed throughout

Table 2. Velocity model (AVM) station corrections, T_c , Argentina aftershock network

| Station | Site Lithology | T_c correction (sec) |
|---------|----------------|---------------------------|
| BRR | Sedimentary | +0.02 |
| CFA | pE rock | +0.30 |
| CHU | do. | +0.32 |
| MAY | do. | +0.35 |
| MOG | Sedimentary | -0.30 |
| SAJ | do. | +0.03 |
| SAM | do. | -0.09 |
| SNO | pE rock | +0.30 |
| VIC | do. | +0.40 |
| VIL | Sedimentary | -0.03 |

the aftershock zone and have depths greater than 10 km.

- b. Locate the selected aftershocks using only the most precise arrival-time data available; that is, the P-wave arrival times from stations located on rock (CFA, VIC, MAY, CHU, and SNO) plus arrival-time data from VIL (for azimuthal control). Assume a P/S velocity ratio of 1.73 and use S-wave arrival times as recorded by the short-period horizontal seismographs at CFA. Apply the AVM station corrections. Results of this location process demonstrated that significant travel time residuals still remained at some stations located on alluvium, particularly MOG, BRR, and SAM. Thus, averages of the travel time residuals were determined for the individual network stations to serve as preliminary delay corrections, T_d .
- c. Relocate the 20 selected events using their above preliminary-delay corrections and the S-wave arrival times recorded at rock site stations and using the Wood-Anderson instruments in San Juan (SAJ). Try various P/S velocity ratios to establish a value that tends to minimize the S-wave residuals and construct a Wadati plot using only the P and S-wave arrival

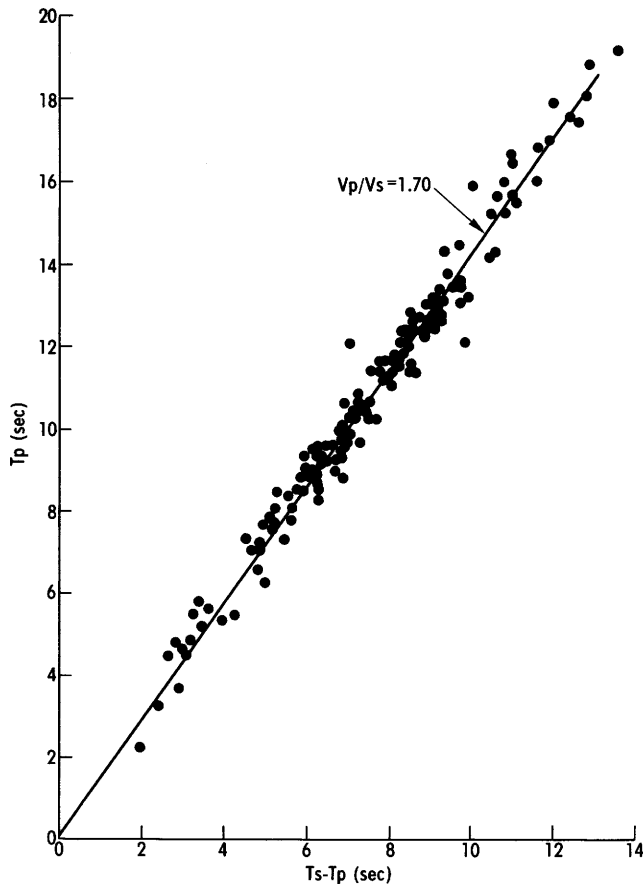


Figure 9. Wadati plot showing traveltimes of S-wave minus traveltimes of P-wave ($T_s - T_p$, sec) versus traveltime of P-wave (T_p , sec) for 20-event subset (refer to page 20). Data from the rock site stations.

times recorded at the rock sites (fig. 9). The result of both the P/S velocity ratio search and the Wadati plot was the selection of a value of 1.70.

- d. To arrive at the final station delay corrections, T_d , relocate the 20-event subset of aftershocks using the 1.70 P/S velocity ratio and average the travel time residuals at each of the 10 stations. Table 3 presents the results of this procedure for the study area.

(4) Final Station Corrections, T_s

Obtain the algebraic sum of the AVM station corrections, T_c , and the "station delay" corrections, T_d , to estimate the "final" station corrections, T_s , as listed in table 4.

SUMMARY

The velocity model described in table 1 and the station corrections listed in table 4 were used in the HYPO71 program to locate the aftershocks of the western

Table 3. Station-delay corrections, T_d Argentina aftershock network

| Station | Site Lithology | T_d Correction (sec) |
|---------|----------------|------------------------|
| BRR | Sedimentary | -0.27 |
| CFA | p# rock | +0.17 |
| CHU | do. | 0.00 |
| MAY | do. | +0.14 |
| MOG | Sedimentary | -0.97 |
| SAJ | do. | 0.00 |
| SAM | do. | -0.39 |
| SNO | p# rock | 0.00 |
| VIC | do. | -0.01 |
| VIL | Sedimentary | +0.38 |

Table 4. Final station corrections, T_s Argentina aftershock network

| Station | Site Lithology | T_s Correction (sec) |
|---------|----------------|------------------------|
| BRR | Sedimentary | -0.25 |
| CFA | p# rock | +0.47 |
| CHU | do. | +0.32 |
| MAY | do. | +0.49 |
| MOG | Sedimentary | -1.27 |
| SAJ | do. | +0.03 |
| SAM | do. | -0.48 |
| SNO | p# rock | +0.30 |
| VIC | do. | +0.39 |
| VIL | Sedimentary | +0.35 |

Argentina earthquake of November 23, 1977 (Langer and Bollinger, 1987). The average HYPO71 error measures for the aftershock hypocentral calculations were: RMS=0.12 sec; ERH=0.7 km; ERZ=1.3 km. We do not have a way to check for the presence of any systematic biases, but the use of high-quality S-wave data from CFA and SAJ eliminates the possibility of gross mislocations. Additionally, the depth distribution of the hypocenters (near surface to 30+ km; 110-135 km) given by Langer and Bollinger is the same as that derived from special seismicity studies of the region (Barazangi and Isacks,

1976). A full listing of the aftershock locational and error parameters is given in the appendix.

ACKNOWLEDGMENTS

Our appreciation is extended to the Instituto Nacional de Prevención Sísmica (INPRES) and all personnel who contributed to our field monitoring program. Director Ing. Julio Aguirve Ruiz and staff seismologist, Dr. Juan C. Castano, provided assistance toward the necessary scientific and logistical support. We are also grateful to S. T. Algermissen for his coordination of this joint U.S.-Argentine postearthquake study. Ing. Abel E. Burna with YPF in Buenos Aires, Argentina, kindly provided the refraction profile data that were so important to our model development. Mr. David R. Toland of Cities Services Corporation, International Area, Houston, Tex., graciously provided the sonic logs for the two wells in the study area.

We also express gratitude to J. P. Whitcomb and R. F. Henrisey for their fieldwork and to Martha Adams, whose careful efforts obtained the basic data from the seismograms. M. J. Cecil and A. M. Rogers critically reviewed the manuscript and provided many helpful comments and suggestions.

REFERENCES CITED

- Allmendinger, R. W., Jordan, T. E., Palma, M., and Isacks, B. L., 1983, Paleogeography and Andean structural geometry, northwest Argentina: *Tectonics*, 2, p. 1-16.
- Baldis, B. A., and Febrer, J., 1983, Geodynamics of the Andean arc and related regions: in *Geodynamics of the Eastern Pacific Region, Caribbean and Scotia Arcs*, edited by Ramon Cabre, S. J., American Geophysical Union and Geological Society of America, Geodynamics Series, v. 9, p. 127-135.
- Barazangi, M., and Isacks, B., 1976, Spatial distribution of earthquakes and subduction of the Nazca plate beneath South America: *Geology*, v. 4, p. 686-692.
- Bastias, H. E., and Weidmann, N., 1983, Mapa de fallamiento moderno de la provincia de San Juan: Universidad Nacional de San Juan, Facultad de Ciencias Exactas, San Juan, Argentina, scale 1:500,000.
- INPRES (Instituto Nacional de Prevención Sísmica), 1977, El terremoto de San Juan del 23 de Noviembre de 1977, informe preliminar: Instituto Nacional de Prevención Sísmica, San Juan, Republica Argentina, 101 p.
- Jordan, T. E., Isacks, B. L., Allmendinger, R. W., Brewer, J. A., Ramos, V. A., and Ando, C. J., 1983, Andean tectonics related to geometry of subducted Nazca plate: *Bulletin of the Geological Society of America*, 94, p. 341-361.
- Kadinsky-Cade, Katherine, Reilinger, Robert and Isacks, Bryan, 1985, Surface deformation associated with the November 23, 1977, Caucete Argentina earthquake sequence: *Journal of Geophysical Research*, v. 90, p. 12,691-12,700.
- Langer, C. J., and Bollinger, G. A., 1988, Aftershocks of the western Argentina (Caucete) earthquake of 23 November 1977—some tectonic implications: *Tectono-physics* (in press).
- Lee, W. H. K., Bennett, R. E. and Meagher, K. L., 1972, A method of estimating magnitude of local earthquakes from signal duration: U.S. Geological Survey Open-File Report 72-223, 28p.
- Volponi, F. S., 1968, Los terremotos de Mendoza del 21 de Octubre de 1968 y la estructura de la corteza terrestre [The Mendoza earthquakes of 21 October 1968 and the structure of the earth's crust]: *Acta Cuyana de Ingenieria*, v. XII, Instituto Sismológico Zonda, Facultad de Ingenieria, Universidad Nacional de Cuyo, San Juan, Argentina, p. 95-110.

APPENDIX

List of aftershocks for the Argentina earthquake of November 23, 1977

| Date (Dec. 1977) | Origin (UTC) | Lat. S (deg) | Long. W (deg) | Depth (km) | No. ¹ obs. | DMIN ² (km) | RMS ³ | Standard errors ⁴ | | | QF ⁵ | M _D | |
|---------------------|-----------------|-----------------|------------------|---------------|--------------------------|---------------------------|------------------|------------------------------|--------------|------------|-----------------|----------------|-----|
| | | | | | | | | DLAT (km) | DLOn (km) | DZ (km) | | | |
| 06 | 1705 | 06.54 | 31.270 | 67.978 | 29.2 | 13 | 45 | 0.09 | .24 | 0.22 | 0.66 | B | 4.7 |
| 06 | 1827 | 39.00 | 31.310 | 67.847 | 24.3 | 11 | 49 | 0.10 | .43 | .31 | 2.35 | C | 4.3 |
| 06 | 1932 | 27.99 | 31.285 | 67.953 | 28.5 | 12 | 45 | 0.13 | .45 | .38 | .73 | B | 3.5 |
| 06 | 2336 | 32.45 | 31.265 | 67.969 | 27.3 | 10 | 46 | 0.08 | .25 | .33 | .95 | B | 3.7 |
| 07 | 0200 | 32.82 | 31.140 | 67.737 | 7.5 | 11 | 47 | 0.08 | .30 | .51 | 2.01 | C | 3.6 |
| 07 | 0322 | 41.52 | 31.276 | 67.956 | 27.8 | 11 | 46 | 0.18 | .56 | .62 | 1.71 | B | 4.4 |
| 07 | 0409 | 55.42 | 31.576 | 67.529 | 13.1 | 12 | 19 | 0.15 | .45 | .57 | 1.80 | B | 3.3 |
| 07 | 0554 | 18.64 | 31.746 | 68.027 | 115.1 | 12 | 6 | 0.11 | .78 | .91 | 1.35 | C | 2.6 |
| 07 | 0655 | 46.13 | 31.694 | 67.939 | 30.0 | 11 | 5 | 0.10 | .61 | .37 | .60 | A | 3.2 |
| 07 | 0802 | 19.84 | 31.837 | 67.836 | 17.7 | 10 | 16 | 0.08 | .28 | .35 | .84 | B | 3.0 |
| 07 | 0807 | 09.89 | 31.038 | 67.803 | 2.4 | 13 | 53 | 0.12 | .24 | .29 | .42 | C | 4.0 |
| 07 | 0817 | 29.49 | 31.827 | 67.737 | 17.1 | 10 | 24 | 0.07 | .21 | .25 | 1.01 | B | 4.1 |
| 07 | 0919 | 04.14 | 31.508 | 67.537 | 52.1 | 12 | 19 | 0.10 | .35 | .43 | .95 | A | 2.5 |
| 07 | 0926 | 12.35 | 31.252 | 67.971 | 22.4 | 12 | 47 | 0.08 | .24 | .22 | 1.75 | B | 2.8 |
| 07 | 0941 | 45.25 | 31.297 | 67.966 | 26.8 | 14 | 43 | 0.12 | .34 | .29 | .83 | B | 3.9 |
| 07 | 1130 | 27.97 | 31.837 | 67.743 | 8.9 | 11 | 24 | 0.09 | .31 | .28 | .81 | B | 2.7 |
| 07 | 1413 | 06.22 | 31.456 | 67.468 | 19.9 | 11 | 15 | 0.17 | .65 | .95 | 2.50 | B | 2.4 |
| 07 | 1431 | 13.52 | 31.128 | 67.881 | 21.6 | 11 | 60 | 0.16 | .50 | .40 | 3.74 | C | 3.4 |
| 07 | 1509 | 39.03 | 31.276 | 67.833 | 21.3 | 11 | 53 | 0.08 | .27 | .28 | 2.17 | C | 3.2 |
| 07 | 1612 | 45.01 | 31.062 | 67.867 | 9.7 | 12 | 58 | 0.09 | .25 | .23 | 2.48 | C | 2.6 |
| 07 | 1705 | 40.21 | 31.580 | 67.734 | 31.1 | 11 | 28 | 0.15 | .55 | .52 | .51 | B | 3.2 |
| 07 | 1720 | 12.82 | 31.822 | 67.808 | 15.0 | 13 | 18 | 0.14 | .32 | .34 | 1.37 | B | 3.1 |
| 07 | 1823 | 48.02 | 31.683 | 67.889 | 30.1 | 11 | 9 | 0.13 | .66 | .66 | .74 | A | 2.8 |
| 07 | 1835 | 12.65 | 31.114 | 67.798 | 7.8 | 14 | 52 | 0.08 | .16 | .19 | .75 | C | 2.7 |
| 07 | 2012 | 27.47 | 31.640 | 67.913 | 28.5 | 11 | 12 | 0.08 | .36 | .24 | .49 | A | 2.9 |
| 07 | 2016 | 14.10 | 31.780 | 67.803 | 22.4 | 12 | 16 | 0.09 | .25 | .25 | .57 | B | 3.1 |
| 07 | 2029 | 13.52 | 31.509 | 67.869 | 22.4 | 11 | 27 | 0.11 | .46 | .32 | 1.47 | B | 3.2 |
| 07 | 2033 | 27.85 | 31.269 | 67.845 | 9.5 | 10 | 53 | 0.13 | .46 | .46 | 4.02 | C | 2.8 |
| 07 | 2137 | 16.22 | 31.043 | 67.782 | 4.4 | 12 | 51 | 0.10 | .23 | .22 | 3.63 | C | 3.2 |
| 07 | 2252 | 29.34 | 31.792 | 67.833 | 21.3 | 11 | 14 | 0.15 | .47 | .47 | .81 | B | 3.0 |
| 08 | 0224 | 36.05 | 31.136 | 67.907 | 23.8 | 12 | 58 | 0.11 | .29 | .30 | 1.27 | C | 2.7 |
| 08 | 0416 | 05.64 | 31.527 | 67.577 | 13.9 | 12 | 23 | 0.07 | .23 | .24 | 1.30 | B | 3.0 |
| 08 | 0625 | 05.09 | 31.231 | 67.803 | 7.9 | 11 | 55 | 0.12 | .38 | .62 | 2.34 | C | 3.3 |
| 08 | 1103 | 28.38 | 31.800 | 67.854 | 24.0 | 11 | 13 | 0.10 | .35 | .42 | .61 | B | 3.2 |
| 08 | 1202 | 26.51 | 31.421 | 67.874 | 7.4 | 10 | 36 | 0.08 | .44 | .31 | 1.79 | B | 3.2 |
| 08 | 1251 | 44.76 | 31.679 | 67.891 | 28.3 | 11 | 10 | 0.16 | .60 | .60 | .89 | B | 2.6 |
| 08 | 1338 | 23.41 | 31.274 | 67.915 | 24.5 | 11 | 48 | 0.13 | .47 | .34 | 2.42 | B | 3.3 |
| 08 | 1505 | 31.44 | 31.077 | 67.853 | 23.8 | 11 | 58 | 0.11 | .33 | .33 | 1.45 | C | 3.2 |
| 08 | 1734 | 21.13 | 31.260 | 67.832 | 2.3 | 10 | 55 | 0.13 | .46 | .31 | .61 | C | 3.0 |
| 08 | 1831 | 47.60 | 31.560 | 67.079 | 134.0 | 13 | 25 | 0.16 | .85 | 1.32 | 1.26 | C | 2.7 |
| 08 | 1834 | 51.93 | 31.285 | 67.966 | 25.8 | 12 | 44 | 0.08 | .20 | .19 | .80 | B | 3.0 |
| 08 | 1904 | 43.57 | 31.458 | 68.022 | 28.2 | 10 | 26 | 0.08 | .31 | .21 | .48 | A | 3.2 |
| 08 | 1952 | 15.33 | 31.234 | 67.752 | 8.0 | 12 | 50 | 0.10 | .22 | .42 | 1.37 | B | 3.8 |
| 08 | 2046 | 35.61 | 31.007 | 67.797 | 5.2 | 12 | 53 | 0.05 | .12 | .12 | .67 | C | 2.5 |
| 08 | 2321 | 28.35 | 31.051 | 67.795 | 19.5 | 13 | 52 | 0.09 | .20 | .30 | 2.89 | C | 2.1 |
| 09 | 0038 | 07.40 | 31.451 | 67.979 | 31.9 | 12 | 30 | .13 | .49 | .37 | .48 | A | 3.3 |
| 09 | 0102 | 28.70 | 31.382 | 67.803 | 8.0 | 11 | 42 | 0.13 | .55 | .33 | 1.52 | B | 3.3 |
| 09 | 0131 | 59.19 | 31.197 | 67.845 | 1.6 | 12 | 58 | 0.18 | .46 | .43 | .71 | C | 2.9 |
| 09 | 0248 | 58.05 | 31.509 | 67.705 | 30.4 | 11 | 35 | 0.09 | .32 | .35 | .38 | B | 3.3 |
| 09 | 0511 | 31.44 | 31.146 | 67.722 | 2.6 | 12 | 45 | 0.06 | .16 | .14 | 2.08 | C | 2.7 |
| 09 | 0716 | 54.56 | 31.058 | 68.003 | 1.7 | 13 | 49 | 0.14 | .26 | .29 | .42 | B | 2.8 |
| 09 | 0825 | 21.78 | 31.034 | 67.800 | 8.0 | 10 | 53 | 0.08 | .23 | .26 | 1.02 | C | 2.7 |
| 09 | 0918 | 12.34 | 31.502 | 67.690 | 31.3 | 11 | 34 | 0.12 | .50 | .39 | .45 | B | 3.0 |
| 09 | 1036 | 03.65 | 31.777 | 67.969 | 10.8 | 12 | 4 | 0.06 | .20 | .15 | .37 | B | 3.3 |
| 09 | 1220 | 11.19 | 31.121 | 67.746 | 7.0 | 13 | 47 | 0.11 | .30 | .42 | 1.51 | B | 2.7 |
| 09 | 1244 | 47.41 | 31.247 | 67.988 | 28.0 | 12 | 46 | 0.18 | .49 | .52 | 1.68 | B | 3.2 |
| 09 | 1519 | 45.19 | 31.272 | 67.980 | 25.6 | 14 | 45 | 0.08 | .20 | .21 | .76 | B | 3.7 |
| 09 | 1842 | 54.79 | 31.098 | 67.864 | 6.5 | 11 | 57 | 0.14 | .46 | .37 | 1.87 | C | 2.3 |
| 09 | 1856 | 09.65 | 31.491 | 67.727 | 31.6 | 11 | 13 | 0.15 | .79 | .58 | .72 | A | 2.7 |
| 09 | 2032 | 27.03 | 30.988 | 67.875 | 9.2 | 13 | 52 | 0.15 | .35 | .38 | 2.94 | C | 3.1 |
| 09 | 2057 | 52.90 | 31.303 | 67.968 | 27.6 | 13 | 42 | 0.12 | .33 | .32 | 1.01 | B | 2.9 |
| 09 | 2144 | 48.19 | 31.615 | 67.839 | 12.8 | 15 | 18 | 0.11 | .27 | .24 | .87 | B | 4.2 |
| 09 | 2247 | 39.93 | 31.348 | 67.868 | 4.8 | 12 | 33 | 0.12 | .42 | .29 | 1.93 | B | 3.8 |
| 09 | 2310 | 48.66 | 31.564 | 67.968 | 30.5 | 12 | 19 | 0.13 | .75 | .52 | .72 | A | 3.3 |

List of aftershocks for the Argentina earthquake of November 23, 1977—Continued

| Date (Dec. 1977) | Origin (UTC) | Lat. S (deg) | Long. W (deg) | Depth (km) | No. ¹ obs. | DMIN ² (km) | RMS ³ | Standard errors ⁴ | | | QF ⁵ | M _D |
|---------------------|-----------------|-----------------|------------------|---------------|--------------------------|---------------------------|------------------|------------------------------|--------------|------------|-----------------|----------------|
| | | | | | | | | DLAT (km) | DLOn (km) | DZ (km) | | |
| 10 | 0030 | 33.21 | 31.416 | 67.908 | 12 | 31 | 0.13 | .49 | .33 | 2.87 | B | 3.1 |
| 10 | 0055 | 22.91 | 31.142 | 67.819 | 14 | 51 | 0.09 | .21 | .18 | .91 | C | 3.0 |
| 10 | 0140 | 25.74 | 31.057 | 68.012 | 14 | 49 | 0.06 | .13 | .19 | .59 | B | 3.5 |
| 10 | 0256 | 41.61 | 31.833 | 67.828 | 12 | 17 | 0.09 | .29 | .33 | .63 | B | 3.2 |
| 10 | 0413 | 19.42 | 31.526 | 67.758 | 12 | 13 | 0.09 | .38 | .25 | .58 | A | 2.9 |
| 10 | 0433 | 57.69 | 30.913 | 69.006 | 16 | 69 | 0.27 | 1.50 | 2.16 | 1.98 | D | 3.6 |
| 10 | 0436 | 18.77 | 31.112 | 67.859 | 15 | 55 | 0.07 | .14 | .13 | .47 | C | 3.1 |
| 10 | 0519 | 38.23 | 31.463 | 67.636 | 12 | 12 | 0.08 | .48 | .28 | 1.02 | A | 3.3 |
| 10 | 0704 | 17.20 | 31.743 | 67.936 | 13 | 3 | 0.10 | .32 | .30 | .30 | B | 3.7 |
| 10 | 0711 | 51.12 | 31.225 | 67.690 | 15 | 39 | 0.12 | .28 | .32 | 1.27 | B | 4.1 |
| 10 | 0719 | 20.84 | 31.135 | 67.771 | 12 | 50 | 0.10 | .26 | .29 | 1.26 | B | 3.3 |
| 10 | 0836 | 56.29 | 31.261 | 67.708 | 12 | 35 | 0.08 | .25 | .28 | 1.42 | B | 4.2 |
| 10 | 1010 | 29.48 | 31.097 | 67.938 | 14 | 56 | 0.08 | .18 | .18 | 1.07 | C | 3.5 |
| 10 | 1016 | 12.99 | 31.579 | 67.849 | 12 | 21 | 0.18 | .78 | .48 | 2.44 | B | 3.8 |
| 10 | 1131 | 07.32 | 31.495 | 67.745 | 12 | 14 | 0.17 | .67 | .47 | .74 | B | 2.8 |
| 10 | 1250 | 13.21 | 31.741 | 67.968 | 10 | 0 | 0.17 | .74 | .70 | .84 | C | 2.8 |
| 10 | 1314 | 05.48 | 31.397 | 68.668 | 17 | 18 | 0.16 | .77 | 1.07 | 1.01 | C | 3.2 |
| 10 | 1419 | 54.63 | 31.249 | 67.735 | 13 | 37 | 0.12 | .39 | .42 | 1.89 | B | 4.0 |
| 10 | 1446 | 29.23 | 31.250 | 67.726 | 13 | 37 | 0.06 | .17 | .21 | 1.39 | B | 3.3 |
| 10 | 1448 | 06.24 | 31.250 | 67.715 | 13 | 36 | 0.14 | .43 | .46 | 2.94 | B | 3.1 |
| 10 | 1504 | 33.02 | 31.615 | 67.959 | 11 | 14 | 0.20 | 1.42 | .96 | 1.24 | B | 2.3 |
| 10 | 1839 | 07.73 | 31.126 | 67.917 | 14 | 56 | 0.13 | .32 | .32 | 1.67 | C | 3.7 |
| 10 | 1926 | 04.85 | 31.856 | 67.705 | 10 | 28 | 0.24 | .74 | 1.09 | 3.99 | B | 3.0 |
| 10 | 1929 | 51.89 | 31.370 | 67.948 | 12 | 37 | 0.19 | .84 | .55 | 3.36 | B | 2.7 |
| 10 | 2047 | 34.09 | 31.778 | 67.490 | 13 | 27 | 0.11 | .31 | .35 | 1.07 | B | 3.3 |
| 10 | 2100 | 19.72 | 31.058 | 67.951 | 11 | 52 | 0.09 | .25 | .22 | .96 | C | 3.5 |
| 10 | 2158 | 07.95 | 31.758 | 67.680 | 12 | 21 | 0.10 | .30 | .29 | .61 | B | 3.4 |
| 10 | 2315 | 10.57 | 31.229 | 67.740 | 13 | 39 | 0.09 | .23 | .28 | 2.16 | B | 3.6 |
| 11 | 0044 | 25.34 | 31.163 | 67.814 | 13 | 48 | 0.12 | .29 | .27 | 1.51 | B | 3.8 |
| 11 | 0327 | 12.73 | 31.038 | 67.802 | 13 | 53 | 0.09 | .30 | .25 | 1.36 | C | 3.3 |
| 11 | 0447 | 31.72 | 31.645 | 68.200 | 13 | 6 | 0.16 | .71 | .84 | 1.80 | C | 2.2 |
| 11 | 0452 | 55.89 | 31.528 | 67.785 | 13 | 15 | 0.09 | .46 | .27 | .37 | A | 2.7 |
| 11 | 0531 | 53.92 | 31.076 | 67.940 | 14 | 55 | 0.09 | .23 | .22 | .98 | C | 3.3 |
| 11 | 0705 | 02.42 | 31.703 | 67.791 | 12 | 17 | 0.14 | .40 | .35 | .77 | B | 3.4 |
| 11 | 0707 | 08.36 | 31.151 | 67.728 | 13 | 46 | 0.06 | .13 | .23 | 2.24 | C | 3.1 |
| 11 | 0758 | 17.41 | 31.271 | 68.757 | 16 | 28 | 0.19 | 1.06 | 1.25 | 1.44 | C | 2.4 |
| 11 | 0945 | 09.35 | 31.168 | 67.788 | 14 | 47 | 0.14 | .29 | .39 | 1.46 | B | 3.4 |
| 11 | 0950 | 36.56 | 31.833 | 67.788 | 9 | 20 | 0.13 | .49 | .60 | 3.01 | C | 2.6 |
| 11 | 0958 | 59.98 | 31.767 | 67.770 | 13 | 19 | 0.09 | .27 | .26 | .65 | B | 3.2 |
| 11 | 1038 | 10.17 | 31.267 | 67.951 | 13 | 45 | 0.08 | .24 | .18 | .73 | B | 3.0 |
| 11 | 1044 | 40.43 | 31.173 | 67.776 | 14 | 46 | 0.07 | .15 | .20 | 2.50 | C | 3.4 |
| 11 | 1046 | 53.67 | 31.080 | 67.891 | 13 | 58 | 0.10 | .28 | .23 | 1.38 | C | 3.0 |
| 11 | 1102 | 12.24 | 31.140 | 67.985 | 11 | 51 | 0.13 | .39 | .40 | 1.55 | B | 3.3 |
| 11 | 1246 | 21.60 | 31.425 | 67.733 | 13 | 19 | 0.10 | .50 | .27 | .73 | B | 2.4 |
| 11 | 1331 | 04.23 | 31.479 | 67.655 | 12 | 10 | 0.11 | .52 | .43 | 1.04 | A | 2.9 |
| 11 | 1402 | 23.51 | 31.277 | 67.893 | 11 | 41 | 0.10 | .28 | .25 | .42 | B | 3.0 |
| 11 | 1430 | 43.87 | 31.366 | 67.728 | 15 | 24 | 0.15 | .42 | .33 | 3.66 | B | 3.0 |
| 11 | 1617 | 11.37 | 31.413 | 67.704 | 14 | 19 | 0.13 | .37 | .31 | .96 | B | 2.9 |
| 11 | 1626 | 00.07 | 31.415 | 67.699 | 13 | 18 | 0.10 | .30 | .26 | 1.97 | B | 3.3 |
| 11 | 1640 | 44.21 | 31.505 | 67.781 | 12 | 16 | 0.13 | .56 | .36 | .87 | A | 3.3 |
| 11 | 1643 | 19.07 | 31.418 | 67.709 | 13 | 18 | 0.11 | .32 | .28 | .79 | B | 3.0 |
| 11 | 1745 | 50.14 | 31.828 | 67.761 | 13 | 22 | 0.09 | .25 | .29 | .60 | B | 2.9 |
| 11 | 1857 | 57.32 | 31.520 | 67.867 | 13 | 23 | 0.19 | .80 | .44 | 3.82 | B | 3.6 |
| 11 | 1934 | 24.03 | 31.116 | 67.856 | 13 | 55 | 0.07 | .18 | .17 | .87 | C | 2.9 |
| 11 | 2121 | 55.83 | 31.538 | 67.730 | 12 | 10 | 0.13 | .60 | .46 | .52 | A | 2.7 |
| 11 | 2128 | 13.25 | 31.084 | 67.816 | 13 | 54 | 0.09 | .20 | .24 | 1.80 | C | 2.6 |
| 11 | 2231 | 59.78 | 31.553 | 67.634 | 12 | 2 | 0.13 | .52 | .46 | .47 | A | 3.1 |
| 11 | 2300 | 56.10 | 31.075 | 67.995 | 14 | 51 | 0.09 | .21 | .21 | 1.21 | C | 2.8 |
| 11 | 2333 | 08.34 | 31.359 | 67.697 | 11 | 24 | 0.20 | 1.00 | .68 | 1.60 | B | 2.9 |
| 12 | 0043 | 29.00 | 31.032 | 67.802 | 12 | 53 | 0.09 | .23 | .23 | .50 | C | 3.8 |
| 12 | 0114 | 45.01 | 31.801 | 67.833 | 13 | 14 | 0.07 | .20 | .22 | .37 | B | 3.6 |
| 12 | 0215 | 38.32 | 31.277 | 67.918 | 12 | 42 | 0.07 | .21 | .19 | .65 | B | 3.5 |
| 12 | 0304 | 45.28 | 31.517 | 68.868 | 16 | 30 | 0.16 | .93 | 1.46 | .95 | C | 2.7 |
| 12 | 0412 | 45.04 | 31.266 | 67.986 | 12 | 45 | 0.10 | .28 | .28 | .94 | B | 2.7 |
| 12 | 0443 | 24.41 | 31.503 | 67.730 | 12 | 12 | 0.05 | .19 | .18 | .19 | A | 2.5 |
| 12 | 0556 | 13.62 | 31.353 | 67.835 | 13 | 31 | 0.12 | .41 | .32 | 2.58 | B | 3.1 |
| 12 | 0611 | 22.57 | 31.466 | 67.666 | 12 | 12 | 0.16 | .63 | .48 | 1.32 | B | 3.3 |
| 12 | 0819 | 52.39 | 31.817 | 67.828 | 11 | 16 | 0.16 | .48 | .60 | 1.54 | C | 2.4 |
| 12 | 0916 | 14.94 | 31.574 | 67.502 | 12 | 12 | 0.09 | .28 | .34 | .86 | B | 2.9 |
| 12 | 1029 | 00.95 | 31.194 | 67.724 | 13 | 43 | 0.14 | .48 | .48 | 2.14 | C | 2.8 |

List of aftershocks for the Argentina earthquake of November 23, 1977—Continued

| Date (Dec. 1977) | Origin (UTC) | Lat. S (deg) | Long. W (deg) | Depth (km) | No. ¹ obs. | DMIN ² (km) | RMS ³ | Standard errors ⁴ | | | QF ⁵ | M _p | |
|---------------------|-----------------|-----------------|------------------|---------------|--------------------------|---------------------------|------------------|------------------------------|--------------|------------|-----------------|----------------|-----|
| | | | | | | | | DLAT (km) | DLOn (km) | DZ (km) | | | |
| 12 | 1244 | 24.77 | 31.120 | 67.779 | 1.6 | 14 | 50 | 0.11 | .22 | .28 | .39 | C | 3.1 |
| 12 | 1342 | 42.09 | 31.208 | 67.694 | 20.0 | 11 | 40 | 0.09 | .34 | .30 | 2.14 | C | 3.1 |
| 12 | 1346 | 00.55 | 31.119 | 67.766 | 2.5 | 12 | 49 | 0.08 | .19 | .19 | 2.89 | C | 2.9 |
| 12 | 1510 | 01.99 | 31.201 | 67.708 | 16.7 | 13 | 41 | 0.13 | .35 | .42 | 3.80 | C | 3.2 |
| 12 | 1517 | 48.25 | 31.392 | 67.864 | 20.9 | 12 | 30 | 0.18 | .71 | .47 | 3.51 | B | 3.0 |
| 12 | 1602 | 29.29 | 31.208 | 67.708 | 20.8 | 14 | 41 | 0.14 | .39 | .50 | 2.85 | B | 3.9 |
| 12 | 1715 | 16.52 | 31.482 | 67.482 | 14.7 | 11 | 15 | 0.09 | .31 | .33 | 1.04 | A | 2.5 |
| 12 | 1748 | 28.64 | 31.198 | 67.698 | 15.7 | 12 | 42 | 0.08 | .28 | .32 | 2.78 | C | 2.9 |
| 12 | 1908 | 36.22 | 31.209 | 67.701 | 24.3 | 12 | 41 | 0.16 | .50 | .56 | 3.15 | B | 2.4 |
| 12 | 2044 | 16.60 | 31.246 | 67.767 | 23.4 | 12 | 38 | 0.13 | .45 | .38 | 3.79 | B | 2.7 |
| 12 | 2056 | 32.39 | 31.577 | 67.720 | 30.8 | 13 | 9 | 0.09 | .24 | .28 | .25 | A | 3.2 |
| 12 | 2307 | 10.58 | 31.566 | 67.922 | 7.0 | 12 | 19 | 0.17 | .58 | .51 | 1.93 | C | 3.2 |
| 12 | 2318 | 23.11 | 31.846 | 67.892 | 19.3 | 13 | 14 | 0.09 | .29 | .28 | .73 | B | 3.7 |
| 12 | 2331 | 51.74 | 31.470 | 67.736 | 30.7 | 12 | 15 | 0.08 | .38 | .32 | .40 | A | 3.0 |
| 13 | 0033 | 09.95 | 31.574 | 67.673 | 5.3 | 14 | 4 | 0.13 | .50 | .36 | 1.10 | B | 3.1 |
| 13 | 0220 | 57.35 | 31.268 | 67.708 | 26.9 | 14 | 34 | 0.14 | .32 | .35 | 1.07 | B | 2.8 |
| 13 | 0304 | 36.21 | 31.385 | 67.702 | 30.3 | 13 | 21 | 0.09 | .33 | .27 | .42 | A | 2.8 |
| 13 | 0341 | 55.31 | 31.222 | 67.753 | 5.7 | 14 | 40 | 0.10 | .32 | .26 | 1.30 | B | 2.9 |
| 13 | 0744 | 12.44 | 31.866 | 67.849 | 18.0 | 12 | 18 | 0.09 | .28 | .31 | .87 | B | 3.5 |
| 13 | 0802 | 11.80 | 31.559 | 67.641 | 34.6 | 12 | 1 | 0.12 | .47 | .44 | .86 | A | 3.1 |
| 13 | 0845 | 40.12 | 31.519 | 67.608 | 34.6 | 13 | 6 | 0.15 | .60 | .53 | .99 | A | 2.3 |
| 13 | 1006 | 17.79 | 31.699 | 67.523 | 23.2 | 14 | 18 | 0.13 | .35 | .39 | .65 | B | 4.3 |
| 13 | 1100 | 26.53 | 31.785 | 67.811 | 9.3 | 11 | 16 | 0.12 | .33 | .46 | .98 | B | 2.7 |
| 13 | 1424 | 04.99 | 31.124 | 67.830 | 7.0 | 13 | 53 | 0.12 | .28 | .34 | 1.54 | C | 3.8 |
| 13 | 1552 | 50.28 | 31.355 | 67.862 | 23.0 | 12 | 32 | 0.15 | .55 | .39 | 2.75 | B | 3.7 |
| 13 | 1620 | 26.83 | 31.231 | 67.772 | 15.2 | 13 | 40 | 0.10 | .29 | .28 | 3.90 | C | 3.6 |
| 13 | 1722 | 54.94 | 31.709 | 67.507 | 16.9 | 13 | 20 | 0.07 | .20 | .19 | .74 | B | 2.7 |
| 13 | 1845 | 45.76 | 31.757 | 67.774 | 21.6 | 11 | 18 | 0.13 | .41 | .36 | .77 | B | 2.7 |
| 13 | 1851 | 45.73 | 31.570 | 67.861 | 12.0 | 12 | 21 | 0.13 | .50 | .29 | 2.18 | B | 3.4 |
| 13 | 1904 | 15.08 | 31.666 | 67.738 | 23.8 | 12 | 15 | 0.15 | .52 | .42 | .85 | B | 2.5 |
| 13 | 1919 | 21.58 | 31.773 | 67.795 | 24.5 | 13 | 17 | 0.09 | .26 | .26 | .52 | B | 2.8 |
| 13 | 2325 | 54.29 | 31.652 | 67.591 | 11.0 | 12 | 10 | 0.06 | .18 | .16 | .81 | B | 3.5 |
| 14 | 0230 | 35.57 | 31.811 | 67.835 | 22.8 | 12 | 15 | 0.13 | .42 | .41 | .79 | B | 2.9 |
| 14 | 0344 | 53.99 | 31.673 | 68.044 | 30.7 | 12 | 10 | 0.15 | .85 | .65 | .59 | C | 2.4 |
| 14 | 0352 | 42.24 | 31.645 | 67.750 | 13.7 | 11 | 14 | 0.10 | .30 | .26 | 1.04 | B | 2.2 |
| 14 | 1124 | 30.31 | 31.139 | 67.911 | 22.6 | 15 | 55 | 0.09 | .19 | .21 | 1.12 | C | 3.2 |
| 14 | 1404 | 11.65 | 31.713 | 67.869 | 29.9 | 12 | 10 | 0.17 | .66 | .57 | .74 | B | 2.4 |
| 14 | 1742 | 55.11 | 31.111 | 67.767 | 8.1 | 12 | 49 | 0.07 | .18 | .22 | .86 | B | 3.1 |
| 14 | 2217 | 08.00 | 31.637 | 69.029 | 116.1 | 16 | 46 | 0.16 | 1.32 | 1.32 | 1.13 | C | 2.9 |
| 15 | 0417 | 25.16 | 31.585 | 67.727 | 29.2 | 14 | 9 | 0.13 | .39 | .36 | .55 | A | 3.0 |
| 15 | 0436 | 33.23 | 31.132 | 67.911 | 8.4 | 13 | 55 | 0.07 | .17 | .17 | 1.41 | C | 3.0 |
| 15 | 0724 | 57.89 | 31.316 | 67.902 | 27.0 | 15 | 38 | 0.11 | .28 | .26 | .88 | B | 3.8 |
| 15 | 0751 | 21.62 | 31.838 | 67.831 | 13.2 | 15 | 17 | 0.11 | .26 | .28 | 1.15 | B | 3.5 |
| 15 | 0803 | 38.56 | 31.493 | 68.722 | 122.2 | 18 | 16 | 0.16 | .86 | 1.15 | .97 | C | 2.8 |
| 15 | 0958 | 24.94 | 31.122 | 67.837 | 6.6 | 14 | 53 | 0.08 | .16 | .16 | .59 | C | 3.7 |
| 15 | 1034 | 02.60 | 31.099 | 67.894 | 22.5 | 14 | 58 | 0.08 | .17 | .19 | .93 | C | 2.9 |
| 15 | 1425 | 40.98 | 31.581 | 67.717 | 29.5 | 12 | 29 | 0.07 | .22 | .23 | .36 | A | 3.2 |
| 15 | 1640 | 23.56 | 31.611 | 67.704 | 29.2 | 12 | 28 | 0.10 | .32 | .33 | .54 | B | 3.3 |
| 15 | 1744 | 59.03 | 31.216 | 67.828 | 5.8 | 12 | 56 | 0.11 | .42 | .29 | 1.74 | C | 3.2 |
| 15 | 1913 | 49.18 | 31.228 | 68.444 | 116.0 | 13 | 12 | 0.09 | .60 | .64 | .91 | B | 2.6 |
| 15 | 2234 | 28.64 | 31.242 | 67.841 | 9.3 | 12 | 41 | 0.06 | .19 | .15 | 1.32 | B | 3.2 |
| 15 | 2258 | 04.85 | 31.831 | 67.847 | 18.1 | 13 | 15 | 0.13 | .36 | .38 | .96 | B | 2.7 |
| 15 | 2320 | 37.86 | 31.194 | 67.719 | 24.2 | 13 | 42 | 0.12 | .29 | .36 | 1.18 | B | 3.2 |
| 16 | 0447 | 02.10 | 31.747 | 68.007 | 28.1 | 13 | 4 | 0.12 | .45 | .42 | .46 | B | 3.2 |
| 16 | 0553 | 01.24 | 31.419 | 67.669 | 33.6 | 12 | 17 | 0.13 | .63 | .48 | 1.59 | A | 3.2 |
| 16 | 1018 | 35.84 | 31.549 | 67.513 | 9.8 | 9 | 11 | 0.25 | 1.37 | 1.41 | 2.50 | C | 2.9 |
| 16 | 1106 | 45.45 | 31.170 | 67.905 | 25.9 | 12 | 51 | 0.09 | .28 | .24 | 1.08 | B | 3.3 |
| 16 | 1215 | 33.30 | 31.461 | 67.617 | 39.1 | 13 | 12 | 0.05 | .25 | .18 | .59 | A | 3.1 |
| 16 | 1249 | 44.28 | 31.798 | 67.939 | 16.5 | 10 | 7 | 0.21 | .91 | .88 | 3.26 | C | 2.9 |
| 17 | 0202 | 37.85 | 31.235 | 67.919 | 26.3 | 13 | 46 | 0.09 | .25 | .22 | .94 | B | 3.7 |

¹No. obs.--the number of observations used to obtain hypocentral solutions.

²DMIN--distance to the closest seismograph station.

³RMS--root mean square errors of travel-time residuals.

⁴Standard errors--the indices of precision relating to the values and distribution of the unknown errors in the hypocentral solution where DLAT=error in latitude, DLOn=error in longitude, and DZ=error in depth.

⁵QF--a measure that is intended to indicate the general reliability of the hypocentral solution where A = excellent epicenter, good focal depth; B=good epicenter, fair focal depth; C=fair epicenter, poor focal depth; D=poor epicenter, poor focal depth.

⁶M_p--Local magnitude estimate of aftershock (Lee and others, 1972).

